Available online at www.sciencedirect.com
SCIENCE DIRECT®
Tetrahedron 60 (2004) 145–158
Tetrahedron

Synthesis and stereochemical studies of di and tetra 9,9′-spirobifluorene porphyrins: new building blocks for catalytic material

Cyril Poriel, Yann Ferrand, Sandrine Juillard, Paul Le Maux and Gérard Simonneaux*

Laboratoire de Chimie Organométallique et Biologique, UMR CNRS 6509 Université de Rennes 1, 35042 Rennes cedex, France

Received 29 July 2003; revised 13 October 2003; accepted 28 October 2003

Abstract—We report the synthesis and stereochemical properties of a new class of molecules containing a covalently-linked porphyrin and spiro-9,9′-bifluorene derivatives. The large spiro substituents hinder rotation about the *meso* position to give atropisomers which can be detected by ^{1}H NMR after phosphine or isocyanide complexation to the ruthenium spiroporphyrins.

1. Introduction

A series of spiro-bridge polymers based on 9,9′-spirobifluorene have been recently synthesized.[1–4] Since the bifluorene rings are orthogonally arranged through a tetracoordinated carbon, it is expected to enhance the rigidity of the polymer and the thermal stability.[2,3] In addition to model receptors for chiral recognition,[5] spiro derivatives provide a potentially useful stereochemistry[6] that makes the molecules suitable for interconnection in future molecular devices.[7,8] Three dimensional polymers can also be prepared by anodic oxidation of spirobifluorenes.[9,10] Giving the importance of these polymers, incorporation of metalloporphyrins to spirobifluorene polymers is an attractive approach to obtain materials for heterogeneous catalysis. The major synthetic challenge is to prepare a pool of monomers containing a covalently-linked porphyrin and a spirobifluorene. Recently, we reported a preliminary communication on a new class of manganese-porphyrin-polymers as heterogeneous oxidation catalysts.[11] In complement to this work, here we report the synthesis of 9,9′-spirobifluorene porphyrins in which spirobifluorene groups have been attached at the *meso* positions.[12] Two generations of porphyrins, di and tetra 9,9′-spirobifluorene porphyrins, were employed to determine the effect of the bulky spirobifluorene groups on the periphery of the porphyrin ring. Thus, the presence of spirobifluorene groups gives substantial steric hindrance and atropisomers can be detected by ^{1}H NMR.

Keywords: Spirobifluorene; Porphyrins; Ruthenium; Atropisomer; Phosphine.
* Corresponding author. Tel.: +33-2-23236285; fax: +33-2-23235637; e-mail address: gerard.simonneaux@univ-rennes1.fr

0040–4020/$ - see front matter © 2003 Elsevier Ltd. All rights reserved.
doi:10.1016/j.tet.2003.10.080

2. Results and discussion

2.1. Synthesis of 9,9′-spirobifluorene-2-carbaldehyde

We decided to explore a method for preparing 9,9′-spirobifluorene-2-carbaldehyde that can be scaled-up to multigram quantities. The synthetic approach to 9,9′-spirobifluorene and then its monoformylated compound is outlined in Scheme 1. 9,9′-Spirobifluorene was prepared from two different ways of synthesis, both of them used 2-iodobiphenyl synthesized from commercially available 2-amino-biphenyl and 9-fluorenone.[13,14] The first way (A), which was described by Tour et al.[13] used a strong base *t*-butyllithium in very drastic conditions has been first tested (Scheme 1). The intermediate 9-(1,1′-biphenyl-2-yl)-9*H*-fluoren-9-ol **2**, obtained before cyclization and dehydratation has been isolated. Thus condensation of 2-iodo-1,1′-biphenyl to 9-fluorenone in *t*-BuLi/pentane solution afforded 9-(1,1′-biphenyl-2-yl)-9-*H*-fluoren-9-ol as an intermediate in 60% yield. Refluxing this intermediate in acetic acid in presence of a few drops of HCl (13N) gave the expected 9,9′-spirobifluorene with 90% yield. However, the second pathway (B) has been preferred giving better yield, in a one pot and mild reaction. This procedure is modified from the one reported by Winter-Werner in 1996.[14]

A general synthesis of monosubstituted derivative of 9,9′spirobifluorene via electrophilic substitution is difficult leading to mixture of di and mono substituted compounds.[15] Monoformylation of the spiro compound to prepare 9,9′-spirobi[fluorene]-2-carbaldehyde **4** was however realized using $TiCl_4/Cl_2CHOCH_3$ reagent with 65% yield. A related route to 9,9′-spirobifluorene-2-carbaldehyde has been recently described with a lower yield (30%).[16]

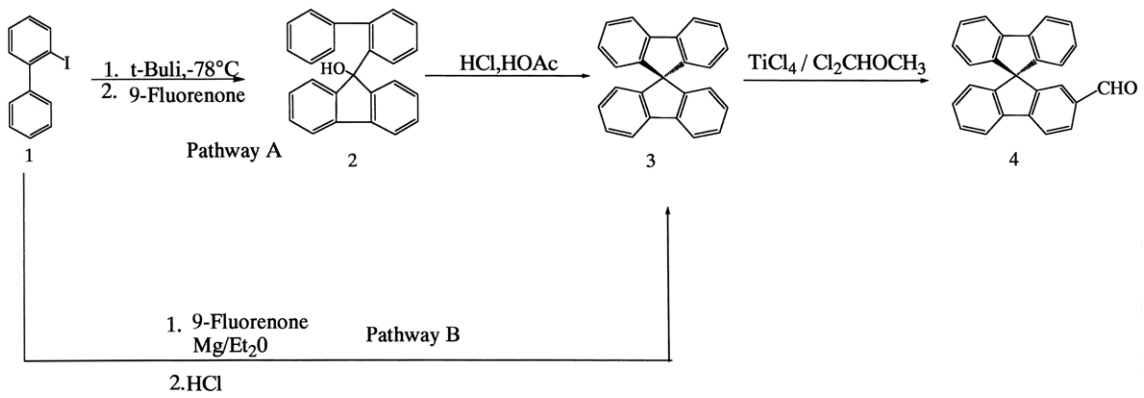

Scheme 1.

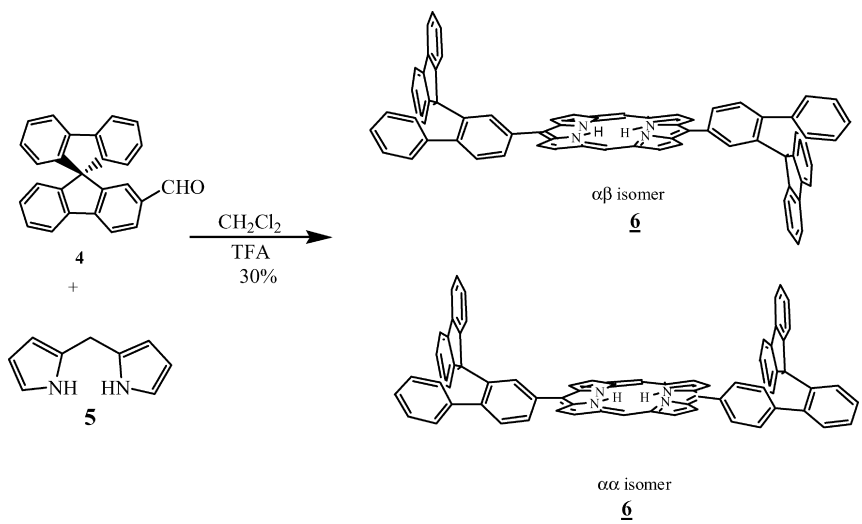

Scheme 2.

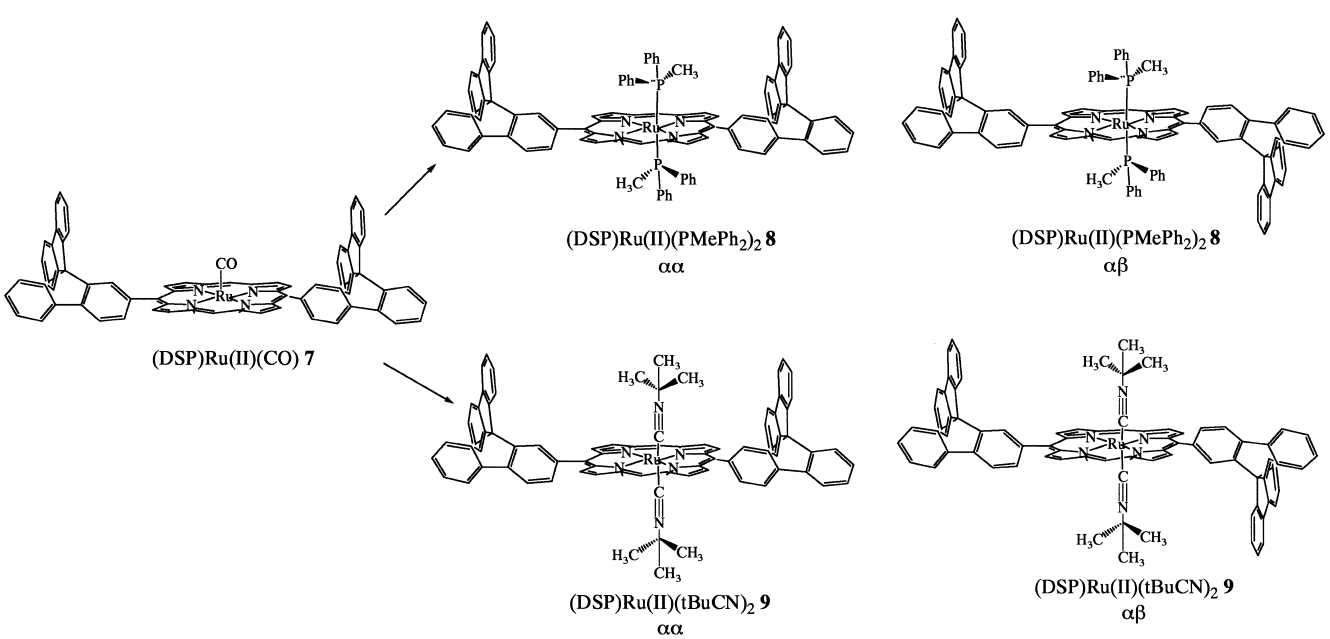

Scheme 3.

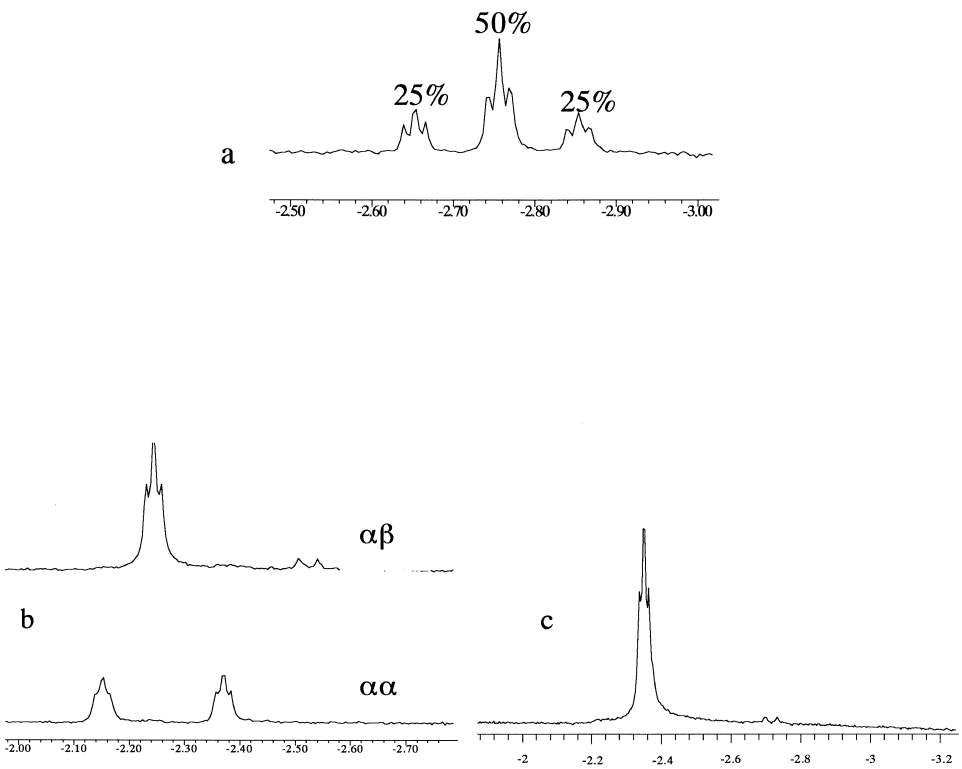

Figure 1. High field portion of the ^{1}H NMR spectrum for compounds **8**, **11** and **12** ($CDCl_3$). (a) Mixture of atropisomers (DSP)Ru(II)$(PMePh_2)_2$ **8**. (b) Separated atropisomers of D(*o*-OMeP)PRu(II)$(PMePh_2)_2$ **11**. (c) D(*m*-OMeP)PRu(II)$(PMePh_2)_2$ **12**.

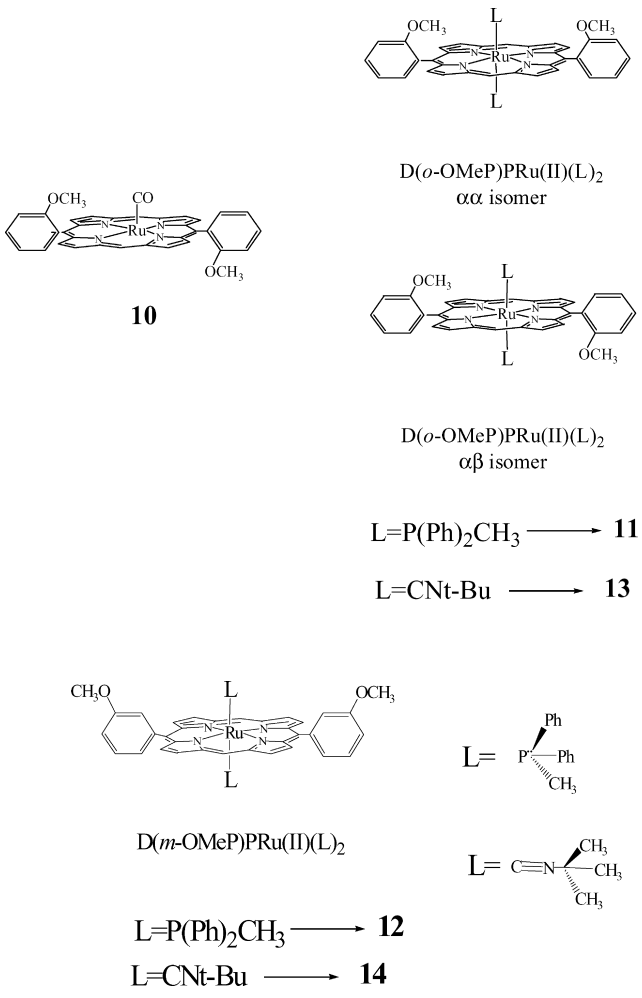

Scheme 4.

2.2. Syntheses of dispiroporphyrins

Due to possible difficulties with the synthesis of tetraspiroporphyrins bearing bulky substituents such as 9,9′-spirobifluorene, we decided first to target porphyrins bearing only two spirobifluorene groups. Such 5,15-disubstituted porphyrins are typically synthesized from a dipyrromethane derivative and an aldehyde.[17,18] This would be expected to yield a mixture of just two porphyrins if there are atropisomers. The bis-5,15-(9,9′-spirobifluoren-2-yl) porphyrin **6** (called DSP for simplication) was synthesized by condensation of 9,9′-spirobifluorene-2-carbaldehyde **4** and dipyrromethane **5**[19] in dichloromethane with trifluoroacetic acid catalysis. A mixture of porphyrins was isolated and separated by column chromatography and found to contain a small amount of monospiroporphyrin along with another porphyrin that we expected to be the dispiroporphyrin. However, identification of this major product was not straightforward. Mass spectrometry gave a molecular ion consistent with **6** but ^{1}H NMR spectroscopy did not give the simple spectra that we have expected. Furthermore this *meso* free porphyrin is insoluble in a variety of common organic solvents such as dichloromethane, chloroform, acetone and dimethylformamide. Due to this strong insolubility, the ^{1}H NMR spectrum was recorded by adding deuterated trifluoroacetic acid steam in the NMR tube. The ^{1}H NMR (500 MHz) spectrum showed an unusual slight splitting of the *meso* and β pyrrole hydrogen according possibly to two rotational isomers (αα and αβ (Scheme 2).

In the αα atropisomer, the substituents attached to the *meso*-aryl groups lie on the same side of the porphyrin plane, in the α,β atropisomer on opposite sides. Although

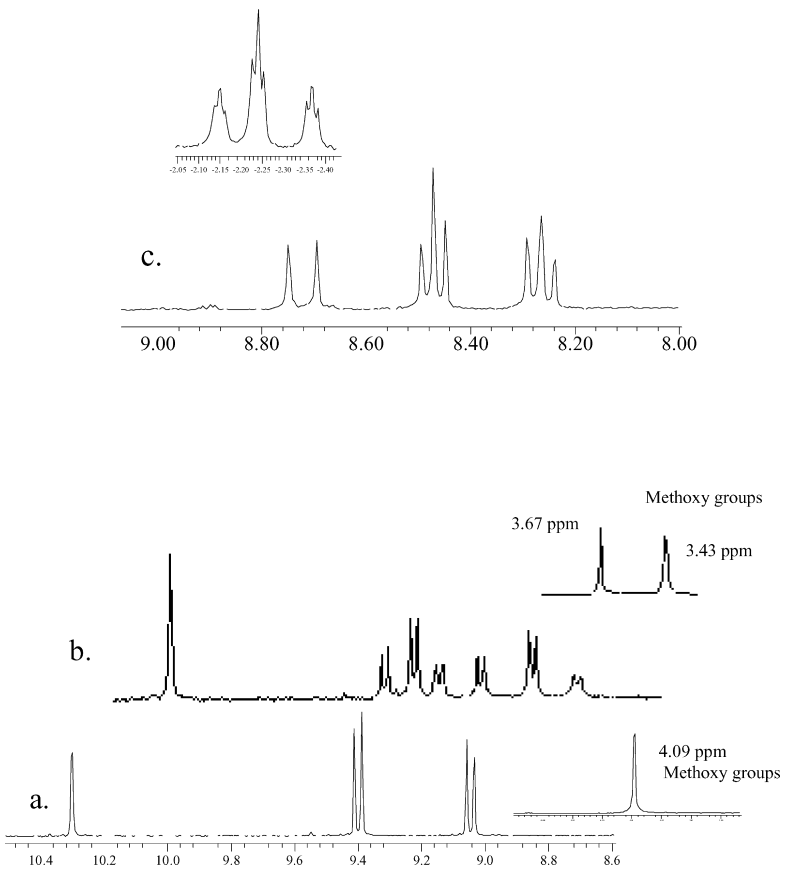

Figure 2. Low field portion of the ^{1}H NMR spectrum: (a) for compound D(*o*-OMeP)PH_2 (αα+αβ); (b) for D(*o*-OMeP)PRu(II)(CO) **10** (αα+αβ); (c) for D(*o*-OMeP)PRu(II)$(PMePh_2)_2$ **11** (αα+αβ) ($CDCl_3$).

atropisomers are not expected when the *meso*-aryl groups are substituted in *meta* position,[20] the large size of the 9,9′-spirobifluorene group may hinder rotation around the $C_{meso}-C_{aryl}$ bond.

2.3. Ruthenium complexation to dispiroporphyrins and stereochemistry

To confirm atropisomerism, the ruthenium complex (DSP)RuII(CO) **7** was first prepared by treatment of **6** with $Ru_3(CO)_{12}$ in highly degassed *o*-dichlorobenzene at 160 °C during 2 h. Then it was decided to study a possible atropisomerism through the complexation of two identical axial ligands. Indeed, complexation of methyldiphenylphosphine or *t*-butylisocyanide offered the greater simplicity because these bis-ligated complexes provided a ruthenium molecule with two topologically identical faces for the α,β isomer and two different faces for the α,α isomer (Scheme 3). The ^{1}H NMR spectrum of the bis(methyldiphenylphosphine) adduct (DSP)Ru(II)$(PMePh_2)_2$ **8** displayed two singlets for the *meso* hydrogens as expected for the presence of two isomers. Moreover the spectrum showed one triplet for the methyl resonance of the axial ligands with the α,β isomer and two triplets of the same intensity for the methyl resonance of $PMePh_2$ for the α,α isomer (Fig. 1(a)). The triplets are due to virtual coupling as reported for similar complexes.[21] These data suggest the presence of a mixture of two conformers, an *anti* (C_{2h} symmetry) and a *syn* isomer (C_{2v} symmetry). It should be underlined that the atropisomerism can also be observed for the *ortho* proton atoms of the phenyl rings of the phosphine ligands for complex **8**.

Since the ^{1}H NMR spectrum showed multiple resonances for the phosphine ligand consistent with atropisomers, variable temperature ^{1}H NMR studies were undertaken to determine the activation energy for aryl rotation in compound **8**. At the coalescence temperature (361 K), free energy of 20.26 kcal/mol was calculated. As recently reported for a porphyrin–carborane system,[22] and a porphyrin–fullerene system,[23] the large size of 9,9′spirobifluorene substituent in meta position increases the energy barrier for aryl rotation; no attempts were made to separate the two atropisomers of compound **8** given the short lifetimes calculated from the activation energy.

To confirm that aryl-porphyrin rotation[24] was the dynamic process being observed, we synthesized the diarylporphyrins bearing methoxy groups in *ortho* position[18] (Scheme 4) and their ruthenium derivatives D(*o*-OMeP)-PRu(II)(CO) **10**. In this case, we were able to separate the mixture of the two atropisomers by silica gel chromatography. As already shown for **6**, the mixture of atropisomers of the free base presented a quite identical ^{1}H NMR (Fig. 2(a)) spectra but the lost of symmetry in the αβ isomer after ruthenium complexation induces a difference in the ^{1}H NMR spectrum (Fig. 2(b)). Indeed the αα isomer exhibits two doublets for β pyrrole protons and four separated doublets can be detected for the αβ isomer in the spectrum.

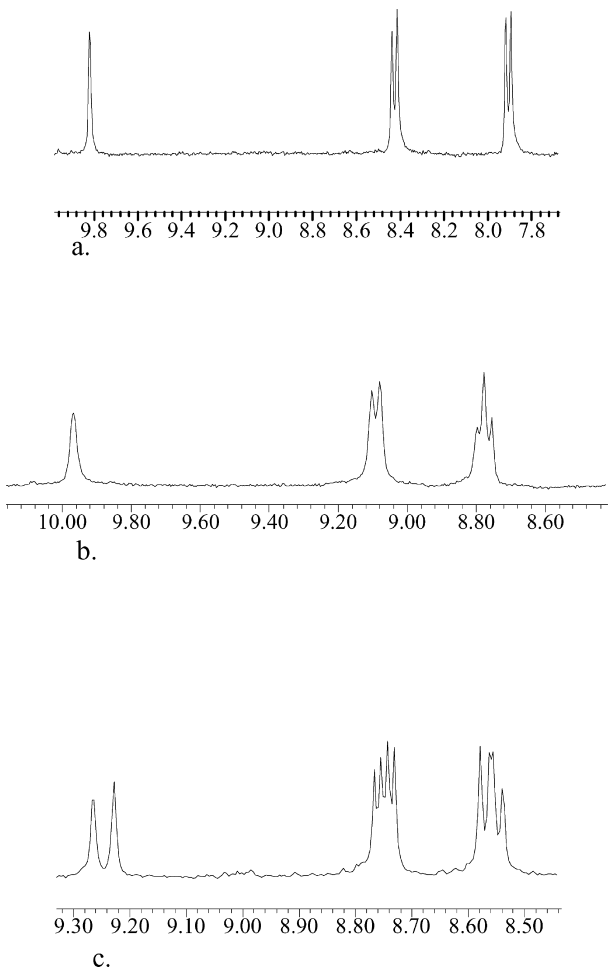

Figure 3. Low field portion of the ^{1}H NMR spectrum: (a) for (DSP)H_2 **6**; (b) for (DSP)RuII(CO) **7**; (c) for (DSP)Ru(II)$(PMePh_2)_2$ **8**.

^{1}H NMR spectrum of the bis(methyldiphenylphosphine) adduct, D(*o*-OMeP)PRu(II) $(PMePh_2)_2$ **11**, was obtained from addition of an excess of ligand to each atropisomer of the D(*o*-OMeP)PRu(II)(CO) precursor **10**. This lead us, in analogy, to assign the two triplets for α,α isomer and the single triplet to the other isomer (Fig. 1(b)). Thermal atropisomerization of each pure isomer in dimethylformamide at 140 °C lead to the statistical mixture 1:1. The synthesis of ruthenium(II) diarylporphyrin complex bearing methoxy groups in *meta* position D(*m*-OMeP)PRu(II)$(PMePh_2)_2$ **12** was also performed. As expected, the spectrum did not show the presence of isomers, displaying only one signal for the methyl group (Fig. 1(c)).

Conformational effect was also established by examining the ^{1}H NMR splitting pattern of the *meso* and pyrrole protons in the low-field part of the spectrum of **8** and **11** which showed two different *meso* protons due to the phosphine complexation (Fig. (3c)). In contrast, only one *meso* proton is detected in **6** and **7** (Fig. (3a,b)).

Observation of phosphorus NMR may be a second possibility to see two different topological faces in theses complexes. The ^{31}P NMR spectra were performed for all the bis phosphine ligated compounds but the sensitivity of this nucleus did not permit to distinguish the different faces of each atropisomer. Indeed, for the (DSP)Ru(II)$(PMePh_2)_2$ **8** complex, only two signals of the same intensity were detected at 2.66 and 2.55 ppm (free ligand: −26.6 ppm), one for αβ isomer and one for the αα isomer. In the later case, the two different faces were not detected by ^{31}P NMR. Such a situation has been already observed for ruthenium picket fence porphyrin.[25]

In order to precise the influence of the steric hindrance caused by the two bulky phenyl groups of the phosphine above the porphyrin ring, *t*-butylisocyanide complexes were also prepared for all compounds previously described. (DSP)Ru(II)(*t*-BuCN)$_2$ **9** was prepared by addition of excess of ligand to the precursor (DSP)Ru(II)(CO) **7** (85%). As expected, the ^{1}H NMR spectrum showed three resonances for the *t*-butyl groups due to the presence of the two conformers (Fig. 4(b)). This complex displayed one singlet for the α,β isomer (−0.70 ppm) and two singlets (−0.57, −0.94 ppm) of the same intensity for the α,α isomer due to inequivalent faces. These results were also compared with the pure αβ and αα D(*o*-OMeP)PRu(II)(*t*-BuCN)$_2$ **13** isomers which exhibit respectively, one and two singlets. As expected, the meta D(*m*-OMeP)PRu(II)(*t*-BuCN)$_2$ complex **14** showed only one singlet for the *t*-butyl groups (Fig. 4(a)).

In order to extend the synthesis and the study of dispiroporphyrins, an other dipyrromethane was synthesized. The choice of 4,4′diethyl-3,3′dimethyl-2,2′dipyrromethane **15** as starting material was not arbitrary. As previously reported by Young and Chang for other *meso*-diphenylporphyrins,[24] the ethyl side chains on β pyrrole

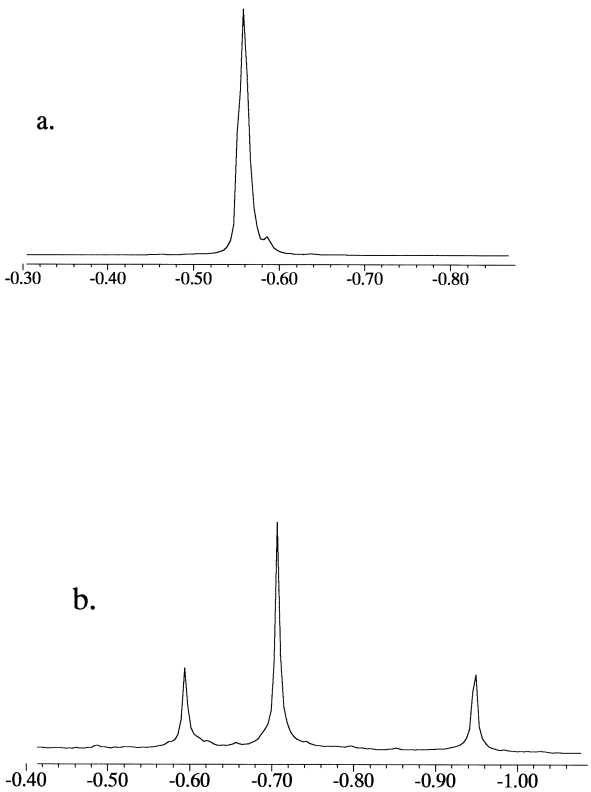

Figure 4. High field portion of the ^{1}H NMR spectrum a for D(*m*-OMeP)PRu(II)(*t*-BuCN)$_2$ **13** and b for (DSP)Ru(II)(*t*-BuCN)$_2$ **9** (mixture of isomers) ($CDCl_3$).

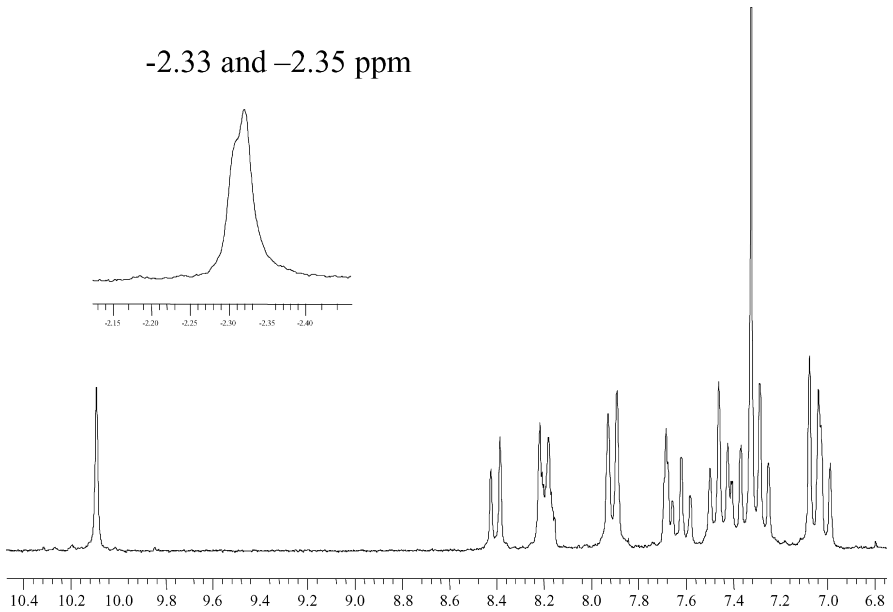

Figure 5. ^{1}H NMR spectrum for compound **16** ($CDCl_3$).

positions rendered dispiroporphyrin more soluble than the non-substituted derivative **6**. Furthermore the methyl group in position 3 constituted a very interesting ^{1}H NMR probe to detect possible atropisomers. Finally, in contrast to previous synthesis of tetramethyldipyrrylmethane,[26] the yields herein were better than 70% in each step.[24]

Mac Donald '2+2' condensation of 4,4′diethyl-3,3′dimethyl-2,2′dipyrromethane **15** with 9,9′-spirobi-[fluorene]-2-carbaldehyde **4** lead to the expected 5,15 bis(spirobifluoren-2-yl)-2,8,18-tetraethyl-3,7,13,17-tetramethyl porphyrin **16** with 40% yield. The increase of solubility compared to porphyrin **6** allowed us to record the ^{1}H NMR spectra of free base **16** in neutral conditions (Fig. 5). The internal NH protons of the porphyrin core were detected as two singlets at −2.33 and −2.35 ppm for the two atropisomers αα and αβ. As expected, signals due to equivalent methyl groups of β pyrrole positions (3, 7, 13 and 17) were separated for each atropisomer (2.16 and 2.17 ppm) and gave a ratio of 1:1 (Scheme 5).

After ruthenium insertion (complex **17**) followed by

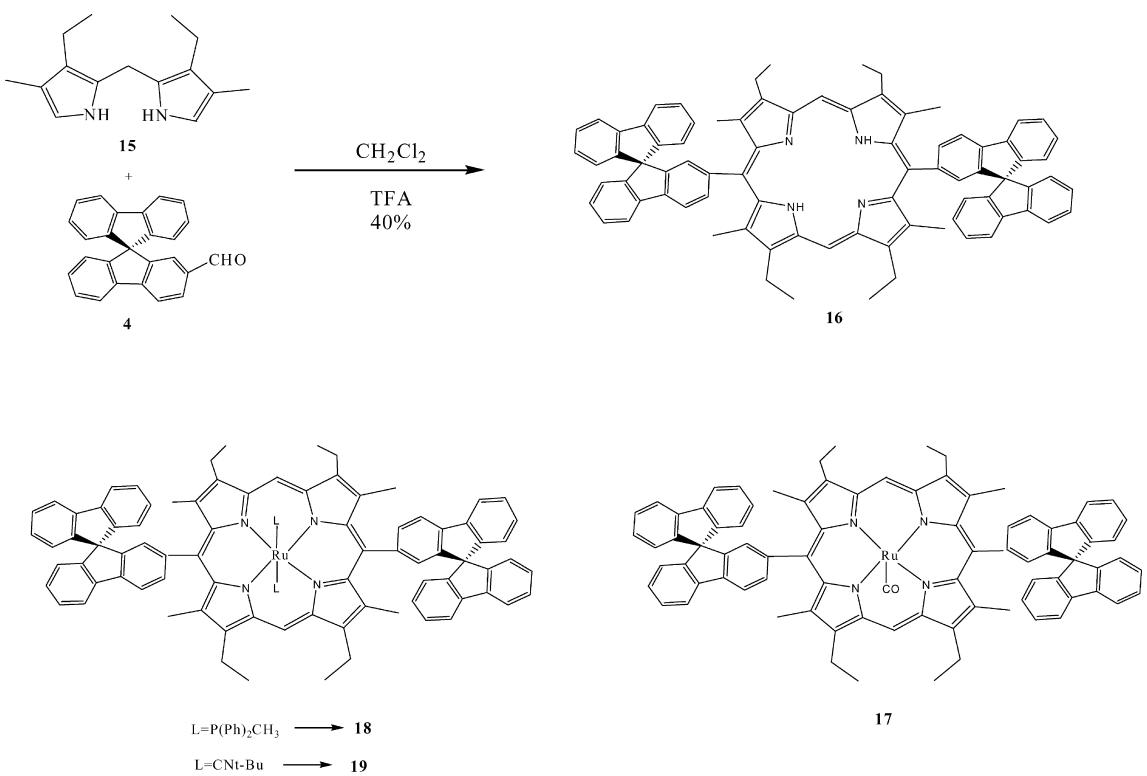

Scheme 5.

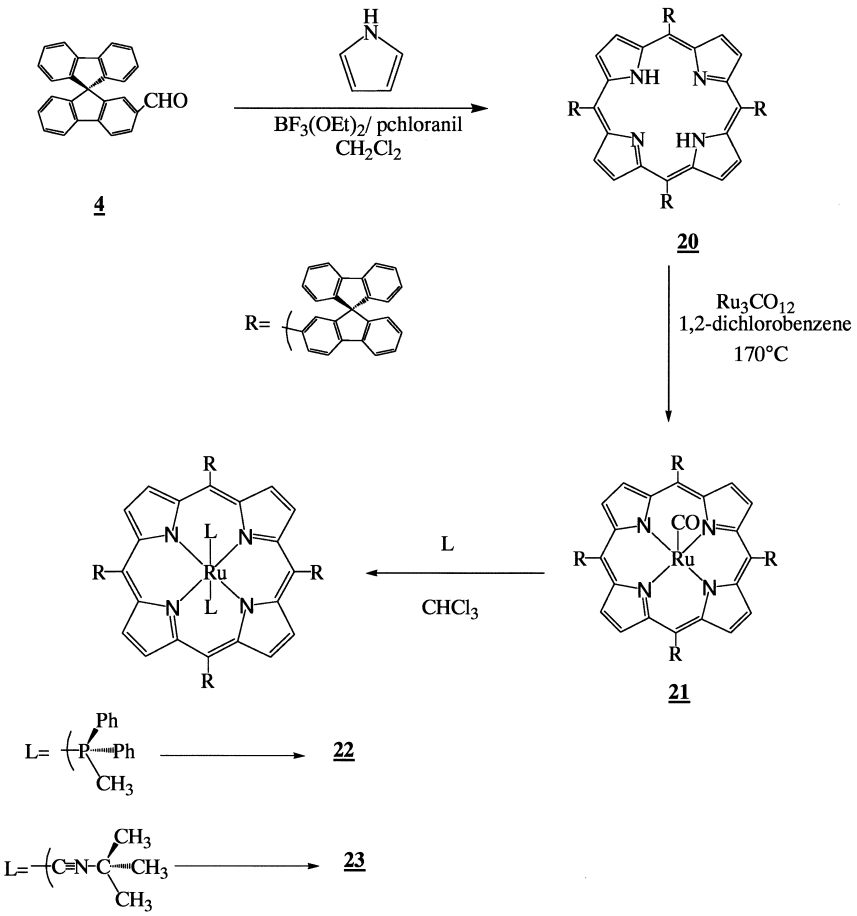

Scheme 6.

phosphine (complex **18**) or isocyanide (complex **19**) complexation, the presence of two different conformers was also detected by ^{1}H NMR. The complex **18** exhibited three resonances at −2.7, −2.54 and −2.30 ppm corresponding to the phosphine methyl groups, and the complex **19** exhibited three resonances at −0.94, −0.70 and −0.58 ppm, corresponding to the isocyanide methyl groups. Variable temperature ^{1}H NMR spectroscopy was applied to quantify the spirobifluorene interaction with the methyl group in β pyrrole position. By monitoring the coalescence of the free *meso* hydrogen in toluene d_8 between 298 and 378 K, ΔG^* at the coalescence temperature (370 K) was estimated as 20.35 kcal mol^{-1}. This allows us to compare the activation free energy ΔG^* for **18** to that for the unsubstituted complex **8**. The activation free energy for rotation in the compound **18** is similar to that for **8** (20.26 kcal/mol) giving rise to a similar energy of rotation around the single bond between porphyrin and spirobifluorene moieties. Intuitively, the addition of flanking alkyl groups should bring more hindrance than the β-pyrrole protons in preventing rotation. However, the absence of an increase in ΔG^* for **18** suggests that this is not true. Therefore the added steric constraints may be not enough to compensate the remote spiro groups in *meta* position. Similar results were previously observed with *ortho* substituents.[24]

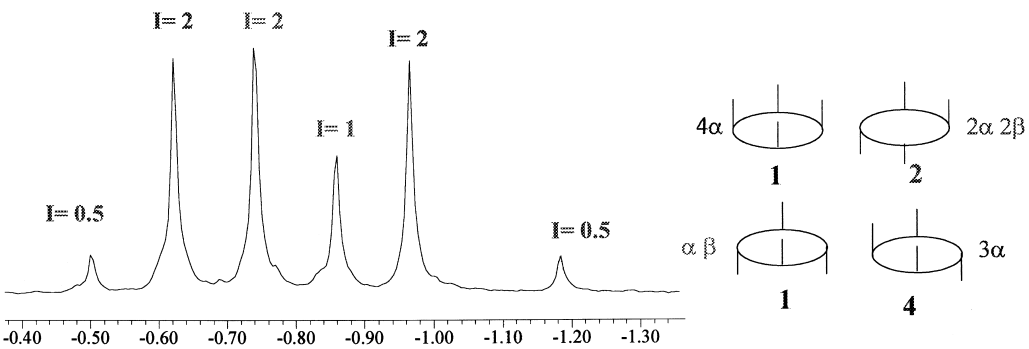

Figure 6. High field portion of the ^{1}H NMR spectrum for compound **23** ($CDCl_3$) with relative intensity of each atropisomer.

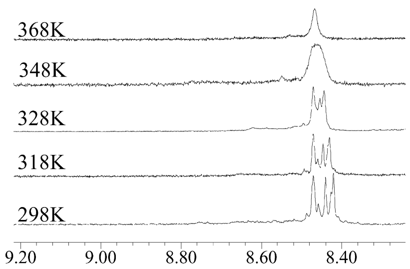

Figure 7. Variable temperature study in toluene d_8 for compound **23** (lowfield part of the spectrum).

2.4. Syntheses and stereochemistry of tetraspiro-porphyrin

Due to weakness of the *meso* free position toward oxidation process, more resistant tetraspirobifluorene porphyrin ruthenium complexes have also been synthesized for further catalytic studies.[27] Following the Lindsey procedure,[19] condensation of 9,9′-spirobifluorene-2-carbaldehyde **4** and pyrrole led to a satisfactory yield (40%) of *meso*-tetra-(m-9,9′-spirobifluoren-2yl)porphyrin **20** (Scheme 6). Indeed, the ^{1}H NMR spectrum of compound **20** displayed several peaks for the pyrrole resonances between 8.74 and 8.68 ppm, and four resonances at high-field position (−2.43, −2.52, −2.54 and −2.56 ppm) assigned to internal NH. Attempts to isolate these free-base atropisomers by classical chromatography techniques were however unsuccessful, due probably to the *meta* position of the bulky spirobifluorene.

After ruthenium insertion (complex **21**) followed by isocyanide complexation (Scheme 6), the presence of four different conformers was also detected by ^{1}H NMR (Fig. 6). The identification of the various isomers in the ^{1}H NMR spectrum of the tetraspirobifluorene porphyrins was based on a combination of two arguments. First the quantities of each isomer present in the equilibrium mixture should correspond to the statistical composition: 1:2:4:1 respectively for αααα, ααββ, αααβ, αβαβ, as we[25] and others[28] have frequently observed. Secondly, two conformers show identical faces whereas the others show different faces. As expected, the spectrum exhibited six resonances found at high-field position due to the ring current shift and with a relative intensity corresponding to the isocyanide methyl groups of the complex **23**. As presented Figure 6, the statistical mixture of four atropisomers was observed. The αααα isomer has two different faces and exhibit two resonances at −1.18 and −0.50 ppm with relative intensity according with its statistical weight. The two topological faces of this isomer are the more different of all the mixture; one bearing the four spirobifluorene groups and the other completely free. This cause a difference of 0.68 ppm between the two resonances; the interpretation and the assignation of all the signals have been made using this argument. The two resonances at −0.96 and −0.62 have been assigned to the αααβ isomer. The ααββ and αβαβ isomer exhibit both two identical faces according to resonances at respectively, −0.74 and −0.86 ppm.

Variable temperature ^{1}H NMR spectroscopy was applied to detect the spirobifluorene interaction with the proton in β pyrrole position for compound **23**, by monitoring the coalescence of the pyrrole hydrogens in toluene d_8 between 298 and 378 K, (Fig. 7). A coalescence temperature was detected near 350 K. The coalescence temperature was 361 K for **8**, suggesting a similar energy of rotation around the single bond between porphyrin and spirobifluorene moieties for the di and tetraspiro derivatives. As already reported for di-*meso*-substituted compounds, comparison with ruthenium tetraphenylporphyrine derivatives bearing on aryl group *meta* substituents was undertaken. Thus, first T(*m*-MeP)PRu(II)$(PPh_2Me)_2$ **26** and then T(*m*-MeP)-PRu(II)(*t*-BuCN)$_2$ **27** were synthesized from the corresponding Ru(II)(CO) derivatives. As expected, the ^{1}H NMR spectrum exhibits only one resonance at high field for the methyl group of the phosphine for **26** and for the methyl of the isocyanide for **27**, respectively (Scheme 7).

3. Conclusion

The phenomenon of atropisomerism in porphyrins with *meso* aryl substituents in ortho position is well known. It was first described in 1969 by Gottwald and Ullman[29] with tetraphenylporphyrins. This concept has been nicely extended first by Collman[28] and then by others[30,31] with

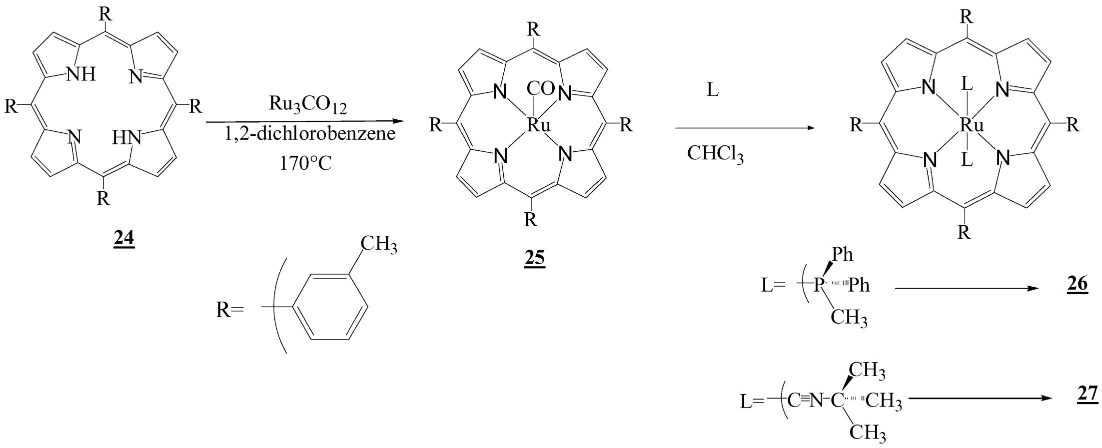

Scheme 7.

meso-tetraaminophenylporphyrins. Since then atropisomerism has also been reported for ortho di-*meso* substituted aryl-porphyrins.[24,32,33] In contrast, *meta*-substitution rarely shows restricted aryl rotation in tetra and di-arylporphyrins. Thus there are only few examples such as porphyrin carborane system,[22] *meta* aryl fullerene porphyrins[23,34] and multimetallic porphyrin monomers.[35] Therefore the large size of the 9,9′-spirobifluorene group also hinders rotation around the $C_{meso}-C_{aryl}$ bond. Unfortunately, energy barrier was too low to get each atropisomer as a pure compounds. In summary, we have developed new efficient syntheses for preparing in mild conditions and with high yield spirobifluorenylporphyrins. These compounds exhibit atropisomers forms which can be easily detected by ^{1}H NMR though the aryl substituents are in *meta* position. Oxidative electropolymerization of tetraspirobifluorenylporphyrin ruthenium (II) carbonyl complexes **21** can be used to coat Pt electrodes with polymeric films as we already reported for manganese-porphyrin-polymers.[11] When unsticked from the electrode, these polymeric ruthenium materials are able to catalyze the heterogeneous cyclopropanations and 2.3 sigmatropic rearrangements with ethyl diazoacetate.[36]

4. Experimental

4.1. General experiments

All reactions were performed under argon and were magnetically stirred. Solvents were distilled from appropriate drying agent prior to use: Et_2O and THF from sodium and benzophenone, toluene from sodium, CH_2Cl_2 from CaH_2, $CHCl_3$ from P_2O_5 and all other solvents were HPLC grade. Commercially available reagents were used without further purification unless otherwise stated. All reactions were monitored by TLC with Merck pre-coated aluminium foil sheets (Silica gel 60 with fluorescent indicator UV_{254}). Compounds were visualized with UV light at 254 and 365 nm. Column chromatography was carried out using silica gel from Merck (0.063–0.200 mm). ^{1}H NMR and ^{13}C NMR in $CDCl_3$ and toluene d_8 were recorded using Bruker (Advance 500dpx, 300dpx and 200dpx) spectrometers. The assignments have been performed by 2D NMR experiments: COSY (Correlation Spectroscopy), HMBC (Heteronuclear Multiple Bond Correlation), HMQC (Heteronuclear Multiple Quantum Coherence) and NOESY (Nuclear Overhauser Effect Spectroscopy). The rates of conformational interchange (k_c) and the activation free energies ΔG^* at the coalescence temperatures were calculated using approximate equation: $k_c=\pi\Delta\nu/(2)^{1/2}$ for the coalescence of singlets.[37] Although the use of this equation can be criticized, it has been shown that the free energies of activation are in good agreement with the results of complete shape analysis based on equally populated two-site system.[37] High-resolution mass spectra were recorded on a ZabSpec TOF Micromass spectrometer for FAB mode or ESI positif mode and on a Varian MAT 311 for EI mode. The spectra were recorded by the CRMPO at the University of Rennes 1. Infrared spectra were recorded on a Bruker IFS 28. Solid samples were prepared in KBr pellets. Liquid samples were prepared in dichloromethane. Melting points were recorded on WME HEIZBANK KOFLER apparatus. UV-visible spectra were recorded on a UVIKON XL from Biotech.

All electrochemical experiments were performed using a Pt disk electrode (diameter 1 mm), the counter electrode was a vitreous carbon rod and the reference electrode was a silver wire in 0.1 M AgNO3 solution in CH_3CN. Ferrocene was added to the electrolyte solution at the end of a series of experiments. The ferrocene/ferricinium (Fc/Fc+) couple served as internal standard and all reported potentials are referenced to its reversible formal potential. The three electrodes cell was connected to a PAR Model 179 signal coulometer. The cyclic voltammetry traces (CVs) were recorded on a XY SEFRAM-type TGM 164. Acetonitrile with less than 5% of water and dichloromethane with less than 100 ppm of water were used without purification. Tetrabutyl ammonium hexafluorophosphate from FLUKA was used without any purification.

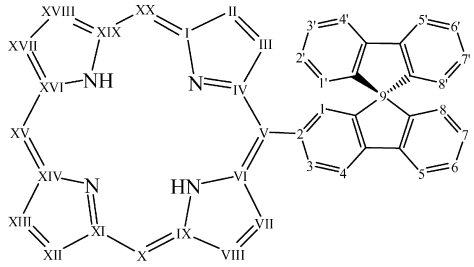

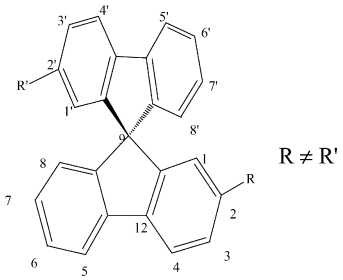

R ≠ R'

4.2. Preparation of spirobifluorene derivatives

4.2.1. 2-Idodo-1,1′-biphenyl 1.[38] To a suspension of 2-amino-1,1′-biphenyl (27 g, 160 mmol) in concentrated hydrochloric acid (32.2 mL) and water (160 mL) cooled at 0 °C was added carefully an aqueous solution of sodium nitrite (13.3 g, 193 mmol) in 10 min. The brown mixture was then stirred at 0 °C for 45 min and added carefully to an aqueous solution of potassium iodide (53.1 g, 320 mmol) in 5 min. The final solution was stirred at room temperature for 12 h and then extracted four times with diethylether. The organic layers were then washed with a solution 3 N of hydrochloric acid, a saturated solution of sodium bicarbonate, sodium chloride, water and dried on magnesium sulphate. The solvents were removed under vacuum to give the 2-idodobiphenyl **1** as purple oil. This compound was used without any other purification (yield: 98%). ^{1}H NMR ($CDCl_3$, ppm): δ 7.1 ($H_{\beta I}$, m, 1H); 7.3–7.6 (m, 7H); 8.03 ($H_{\alpha I}$, m, 1H). ^{13}C NMR ($CDCl_3$, ppm): δ 99.3; 128.2; 128.3; 128.6; 128.8; 129.4; 129.9; 130.7; 131.5; 140.1; 144.7; 147.2. MS (EI) (*m*/*z*): calcd for $C_{12}H_9I$ (M^{+}): 279.97490. Found: 279.9748.

The synthesis of 9,9′-spirobifluorene **3** which was previously described by Tour et al.[13] is not described here. However the spectroscopic data of the intermediate 9-(1,1′-biphenyl-2-yl)-9*H*-fluoren-9-ol **2** are reported.

4.2.2. 9-(1,1′-Biphenyl-2-yl)-9*H*-fluoren-9-ol 2. ^{1}H NMR ($CDCl_3$, ppm): δ 2.28 (OH, s, 1H); 6.01 (dd, 4H); 6.62 (td, 4H); 6.92 (m, 4H); 7.34 (td 1H); 7.6 (td, 2H); 8.1 (dd, 2H). ^{13}C NMR ($CDCl_3$, ppm): δ 82.88; 120.51; 124.79; 125.55; 126.55; 126.71; 127.32; 127.54; 128.35; 129.10; 129.32; 131.7; 140.14; 140.65; 140.79; 151.02. MS (EI) (*m*/*z*): calcd for $C_{25}H_{18}O$ ($M^{\cdot+}$): 334.13577. Found: 334.1368. Mp: 180 °C.

4.2.3. 9,9′-Spirobifluorene 3. Under argon atmosphere 2-iodo-1,1′-biphenyl **1** (44.3 g, 158 mmol) was added dropwise in 30 mn to magnesium turning (5 g, 205 mmol) in 100 mL of diethylether freshly distilled. The addition was controlled to maintained a gentle reflux of diethylether. The mixture was heated to reflux for 90 min and then diluted with 100 mL of diethylether. The mixture was then filtered under argon atmosphere and a solution of 9-fluorenone (37 g, 205 mmol) dissolved in 300 mL of toluene was added dropwise. The mixture was heated to reflux for 24 h. After cooling, the solution was added to 250 g of crushed ice, diluted with 200 mL of toluene and finally 300 mL of concentrated hydrochloric acid was carefully added in 5 min. The solution was stirred for 3 h at room temperature. The two layers were separated and the aqueous layer extracted with dichloromethane. The organic layers were then washed with a saturated solution of sodium bicarbonate, sodium chloride, and water and dried on magnesium sulphate. The solvents were removed under vacuum and the crude product was purified by chromatography on silica gel (first: pentane, second: pentane with a gradient of dichloromethane (from 1 to 30%). Finally the 9,9′-spirobifluorene **3** was washed with a few amount of cold ethanol to afford a white powder (yield: 90%). ^{1}H NMR ($CDCl_3$, ppm): δ 6.79 (H_1, dd, 4H); 7.16 (H_2, td, 4H); 7.42 (H_3, td, 4H); 7.91 (H_4, dd, 4H). ^{13}C NMR ($CDCl_3$, ppm): δ 66 (C_9); 119.87; 123.9; 127.6; 127.7; 141.6; 148.6 (aromatic C). MS (FAB) (*m*/*z*): calcd for $C_{25}H_{16}$ ($M^{\cdot+}$): 316.1252. Found: 316.1249. UV–VIS (CH_2Cl_2): $\lambda_{max/nm}$ (log ε): 225 (4.79); 236 (4.59); 261 (4.51); 294 (4.11); 305 (4;34). Mp: 202°C. CV (CH_2Cl_2 0.2 M/Bu_4NPF_6, Fc/Fc^+): 1.3 V; 1.42 V.

4.2.4. 9,9′-Spirobifluorene-2-carbaldehyde 4. To a solution of 9,9′-spirobifluorene (12.7 mmol) in 100 mL of distilled and degassed dichloromethane, cooled at 0 °C, was added α,α-dichloro-methyl-methylether (31.6 mmol) in one portion. After 5 min titanium tetrachloride (31.6 mmol in 50 mL dichloromethane) was added drop wise over a period of 45 min. The dark green solution was then stirred at room temperature for 75 min and 250 g of ice was then added and let under vigorous stirring for 30 min. The two layers were then separated and the aqueous layer was extracted two times with 100 mL of dichloromethane. The organic layers were then washed with a saturated solution of sodium bicarbonate, sodium chloride, and water and dried on magnesium sulphate. The solvents were removed under vacuum and the crude product was purified by chromatography on silica gel ($CHCl_3$/Pentane: 6/4) (yield: 65%). ^{1}H NMR (500 MHz, $CDCl_3$): δ 6.74 ($H_{1'}$, ddd, 2H), 6.82 (H_8, ddd, 1H), 7.14 ($H_{2'}$, td, 2H), 7.22 (H_7, td, 1H), 7.30 (H_1, sdd, 1H), 7.43 ($H_{3'}$, td, 2H), 7.47 (H_6, td, 1H), 7.91 ($H_{4'}$, ddd, 2H), 7.94 (H_3, dd, 1H), 7.96 (H_5, ddd, 1H), 8.04 (H_4, dd, 1H), 9.84 (CHO, s, 1H). ^{13}C NMR (75 MHz, $CDCl_3$): δ 65.6 (C_9); 120.2; 120.3; 121.1; 123.8; 124.3; 124.5; 125.2; 127.9; 128; 129.5; 130.2; 135.9; 140.1; 141.8; 147.4; 147.8; 149.7; 150 (C aromatic); 191.6 (C═O). UV–VIS (CH_2Cl_2): $\lambda_{max/nm}$ (log ε): 225 (4.59), 282 (4.31), 292 (4.32), 303 (4.38), 328 (4.08). MS (FAB) (*m*/*z*): calcd for $C_{26}H_{16}O$ ($M^{\cdot+}$): 344.1201. Found: 344.1199. Mp: 209 °C. CV (CH_2Cl_2 0.2 M/Bu_4NPF_6, Fc/Fc^+): 1.34 V, 1.66 V.

4.2.5. 2,2′ Dipyrromethane 5. The 2,2′-dipyrromethane **5** was prepared according to the literature procedure and use without other purification (yield: 35%).[19] ^{1}H NMR ($CDCl_3$, ppm): δ 4.01 (CH_2C_2, s, 2H); 6.14 (CH, m, 2H); 6.24 (CH, m, 2H); 6.65 (CH, m, 2H); 7.90 (NH, s br, 2H). MS (EI) (*m*/*z*): calcd for $C_9H_{10}N_2$ ($M^{\cdot+}$):146.0844. Found: 146.0849.

4.2.6. 4,4′-Diethyl-3,3′-dimethyl-2,2′-dipyrromethane 15. 5,5′-Bis(ethoxycarbonyl)-4,4′-diethyl-3,3′-dimethyl-2,2′-dipyrromethane (5.3 mmol) which was obtained from pentan-2,4-dione as previously reported by Lash[39] was dissolved at 100 °C in ethylene glycol (20 mL). The orange solution was degassed for 15 min before adding sodium hydroxide (53 mmol) and heated at 180 °C under an argon atmosphere for 1 h. The mixture was diluted with water and extracted several times with hexane. The organic layers were concentrated, dried over magnesium sulphate and evaporated under reduce pressure. 4,4′-diethyl-3,3′-dimethyl-2,2′-dipyrromethane **15** was stored and protected from light, under an argon atmosphere at −10 °C and used without other purification (yield: 70%). ^{1}H NMR ($CDCl_3$, ppm): δ 1.33 (CH_3C_3, t, 6H); 2.27 (CH_3C_4, s, 6H); 2.67 (CH_2C_3, q, 4H); 3.95 (CH_2C_2, s, 2H); 6.43 (CHC_5, s, 2H); 7.31 (NH, s, 2H). MS (EI) (*m*/*z*): calcd for $C_{15}H_{22}N_2$ ($M^{\cdot+}$): 230.1783. Found: 230.1763.

4.2.7. 5,15-Bis(9,9′-spirobifluoren-2-yl) porphyrin 6. A solution of 2,2′-dipyrromethane **5** (225 mg, 1.54 mmol) and 9,9′-spirobifluorene-2-carbaldehyde **4** (530 mg, 1.54 mmol) in freshly distilled dichloromethane was degassed 10 min. Trifluoroacetic acid (95 μL, 1.22 mmol) was added and the reaction mixture was stirred and protected from light under an argon atmosphere for 15 h. 2.1 mmol (520 mg) of tetrachlorobenzoquinone was added to irreversibly oxidize the di-spiroporphyrinogene and the solution was stirred at air for 60 min and 30 min to reflux. After addition of several drops of triethylamine and the ordinary work-up, concentration, washing, drying, the crude reaction mixture was purified by chromatography on silica gel respectively, with diethyl ether, dichloromethane, mixture of dichloromethane/methanol (8:2) and dichloromethane saturated with concentrated hydrochloric acid. These two last fractions were evaporated and washed with a saturated solution of sodium bicarbonate, sodium chloride, and water and dried on magnesium sulphate. The crude product was dissolved in dichloromethane saturated with concentrated hydrochloric acid and a second chromatography was performed using the same solvents. The last green fraction afforded pure protonated 5,15-bis(9,9′-spirobifluoren-2-yl) porphyrin **6**. The previous work up was performed, the

solvent was removed under vacuum and **6** was crystallized in pentane (yield: 30%). ^{1}H NMR ($CDCl_3$/TFA, ppm) (αα and αβ): δ 7.01 (H_8, dd, 2H); 7.12 ($H_{1'}$, dd, 4H); 7.32 ($H_{2'}$, td, 4H); 7.36 (H_7, td, 2H); 7.5 ($H_{3'}$, td, 4H); 7.6 (H_6, td, 2H); 7.91 (H_1, sd, 2H); 7.94 ($H_{4'}$, dd, 4H); 8.2 (H_5, dd, 2H); 8.41 (H_3, dd, 2H); 8.43 (H_4, dd, 2H); 8.73 ($H_{III,VII,XIII,XVII}$, β pyrrole, d, ^3J=4.83 Hz, 4H); 9.25 ($H_{II,VIII,XII,XVIII}$, β pyrrole, d, ^3J=4.82 Hz, 4H); 10.66 ($H_{X,XX}$ *meso*, s, 2H). ^{13}C NMR ($CDCl_3$/TFA, ppm): δ 66.3 (C_9); 106.6 ($C_{X,XX}$ *meso*); 119.8; 120.5 (C_4); 121.1 ($C_{4'}$); 121.8 (C_5); 124.3 ($C_{1'}$); 125 (C_8); 128.5 ($C_{3'}$); 128.6 ($C_{2'}$); 128.7 (C_6); 129.2 ($C_{II,VIII,XII,XVIII}$, β pyrrole); 129.6 (C_7); 129.8 ($C_{III,VII,XIII,XVII}$, β pyrrole); 133.8 (C_1); 139.7; 140 (C_3); 142; 142.5; 142.7 ($C_{I,IX,XI,XIX}$); 143.7; 146.5 ($C_{IV,VI,XIV,XVI}$); 148; 149.8; 150 (NMR experiments have been performed by adding TFA in the NMR tube due to the insolubility of free base **6**). MS (FAB) (*m*/*z*): calculated for $C_{70}H_{43}N_4$ $(M+H)^+$: 939.3488. Found: 939.3477. UV–VIS (CH_2Cl_2): $\lambda_{max/nm}$ (log ε): 227 (4.62); 297 (4.13); 307 (4.16); 412 (5.11); 505 (3.92); 541 (3.85); 575 (3.51); 632 (3.38).

4.2.8. 5,15-Bis(9,9′-spirobifluoren-2-yl)-2,8,12,18-tetraethyl-3,7,13,17-tetramethylporphyrin 16. A solution of 4,4′-diethyl-3,3′-dimethyl-2,2′-dipyrromethane **15** (354.2 mg, 1.54 mmol) and 9,9′-spirobifluorene-2-carbaldehyde **4** (530 mg, 1.54 mmol) in freshly distilled dichloromethane was degassed 10 min. Trifluoroacetic acid (95 μL, 1.22 mmol) was added and the reaction mixture was stirred protected from light under an argon atmosphere for 15 h, 2.1 mmol (520 mg) of tetrachlorobenzoquinone was added to irreversibly oxidize the di-spiroporphyrinogene and the solution was stirred in air at room temperature for 60 min and then 30 min in refluxing solvent. After addition of several drops of triethylamine and the ordinary work-up, concentration, washing, drying, the crude reaction mixture was purified by chromatography on silica gel (yield: 40%). ^{1}H NMR ($CDCl_3$/TFA, ppm) (αα and αβ): δ −2.35 (NH, s, 1H); −2.33 (NH, s, 1H); 1.30 (CH_3 ethyl, t, 12H); 2.16 (CH_3 methyl, s, 6H); 2.17 (CH_3 methyl, s, 6H); 3.62 (CH_2 ethyl, q, 8H); 6.99 (H spirobifluorene, m, 6H); 7.2–7.45 (H spirobifluorene, m, 10H); 7.59 (H spirobifluorene, m, 4H); 7.85 (H spirobifluorene, dd, 4H); 8.14 (H spirobifluorene, m, 4H); 8.35 (H spirobifluorene, dd, 2H); 10.07 ($H_{X,XX}$ *meso*, s, 2H). MS (ESI: CH_2Cl_2/MeOH: 9/1) (*m*/*z*): calcd for $C_{82}H_{67}N_4$ $(M+H)^+$: 1107, 5366. Found: 1107, 5375. UV–VIS (CH_2Cl_2): $\lambda_{max/nm}$ (log ε): 227 (4.60); 297 (4.10); 307 (4.13); 410 (5.13); 508 (3.90); 543 (3.81); 577 (3.44); 634 (3.30).

4.2.9. *meso*-5,10,15,20-Tetrakis (9,9′-spirobifluoren-2-yl) porphyrin 20. Pyrrole (524 μL, 7.5 mmol) and 9,9′-spirobifluorene-2-carbaldehyde **4** (2.5 g, 7.5 mmol) were allowed to react at room temperature in dry and degassed dichloromethane (750 mL) under an argon atmosphere and protected from light with trace acid catalysis ($BF_3(OEt)_2$ 48%: 0.75 mmol). Under these conditions, the reaction reaches equilibrium in about 3 h. 6.25 mmol (1.54 g) of p-chloranil was added to irreversibly oxidize the tetraspiroporphyrinogene and the solution was stirred at air for 60 and 30 min to reflux. After addition of several drops of triethylamine and the ordinary work-up, concentration, washing, drying, the crude reaction mixture was purified by chromatography twice on silica gel: first with dichloromethane and then with cyclohexane/dichloromethane: 1/3. Crystallization in distilled toluene for one night at room temperature afforded a purple powder of *meso*-tetrakis 5,10,15,20-(spirobifluoren-2-yl) porphyrin (yield: 40%). ^{1}H NMR ($CDCl_3$, ppm) (4α, 3αβ, 2α2β, αβαβ): δ-3.13 (s, 2H, NH); 6.88 (H_8, d, 4H); 7.07 ($H_{1'}$, m, 8H); 7.21 ($H_{2'}$/H_7, m, 12H), 7.32 ($H_{3'}$, m, 8H); 7.50 (H_6+H_1, m, 8H); 7.71 ($H_{4'}$, m, 8H); 8.07–8.15 (H_5/H_4/H_3, m, 12H); 8.55 (H β pyrrole, m, 4H); 8.57 (H β pyrrole, m, 4H). ^{13}C NMR ($CDCl_3$, ppm): δ 66.1 (C_9); 118; 119.8; 120.1; 120.3; 123.9; 124.2; 127.7; 127.9; 128.1; 128.2; 129; 131(C β pyrrole); 134.9; 141.2; 141.5; 141.7; 141.8; 147.4; 147.6; 148.7; 149.6. MS (FAB) (*m*/*z*): calcd for $C_{120}H_{71}N_4$ $(M+H)^+$: 1567.5634. Found: 1567.5600. UV–VIS (CH_2Cl_2): $\lambda_{max/nm}$ (log ε): 228 (5.08); 297 (4.58); 309 (4.67); 427 (5.32); 520 (4.17); 556 (4.09); 594 (3.74); 652 (3.76). CV (CH_2Cl_2 0.2 M/Bu_4NPF_6, Fc/Fc^+): 0.585; 0.915; 1.395 (sh); 1.505.

4.3. Typical procedure for ruthenium insertion

Free base porphyrin (313 μmol) was dissolved in distilled 1,2-dichlorobenzene and degassed for 15 min. The reaction mixture was heated at 160 °C and dodecacarbonyl triruthenium was added (830 μmol) over a period of 2 h under an argon atmosphere. The ruthenium insertion was followed by TLC and UV–Vis spectroscopy. The solvents were removed under vacuum, the residue was dissolved in dichloromethane and purified by chromatography on silica gel. The dodecacarbonyl triruthenium was eluted first with pentane and the desired ruthenium complex was eluted with a mixture dichloromethane/diethylether (9:1). Ru(II)(CO) complex was further crystallized from pentane–dichloromethane.

4.3.1. 5,15-Bis(9,9′-spirobifluoren-2-yl) porphyrinato ruthenium carbonyl 7. Yield: 76%. ^{1}H NMR ($CDCl_3$, ppm) (αα and αβ): δ 6.88 (H spirobifluorene, dd, 2H); 7.1–7.26 (H spirobifluorene, m, 8H); 7.29–7.38 (H spirobifluorene, m, 6H); 7.54 (H spirobifluorene, m, 4H); 7.73 (H spirobifluorene, m, 4H); 8.11–8.29 (H spirobifluorene, m, 6H); 8.72 (H β pyrrole, d, 2H); 8.75 (H β pyrrole, m, 2H); 9.04 (H β pyrrole, d, 4H); 9.93 ($H_{X,XX}$ *meso*, s, 2H). MS (FAB) (*m*/*z*): calcd for $C_{71}H_{41}N_4O^{102}Ru$ $(M+H)^+$: 1067.2344. Found: 1067.2349. UV–VIS (CH_2Cl_2): $\lambda_{max/nm}$ (log ε): 228 (4.80); 296 (4.40); 308 (4.50); 404 (5.11); 521 (4.02); 552 (3.58). IR (KBr, cm^{-1}): ν_{CO} 1943.

4.3.2. 5,15-Bis(2-methoxyphenyl) porphyrinato ruthenium carbonyl 10. Yield: 70%. The free base compound has been synthesized according the procedure described by Manka and Lawrence.[18]

^{1}H NMR ($CDCl_3$, ppm) (αβ isomer): δ 3.45 (s, 6H, methyl group); 7.25–8 (m, 8H, H phenyl ring); 8.54 (Hβ pyrrole, d, ^3J=4.5 Hz, 2H); 8.87 (Hβ pyrrole, d, ^3J=4.6 Hz, 2H); 9.02 (Hβ pyrrole, d, ^3J=4.6 Hz, 2H); 9.25 (Hβ pyrrole, d, ^3J=4.8 Hz, 2H); 10.02 (H *meso*, s, 2H). (αα isomer): δ 3.6 (s, 6H, methyl group); 7.25–8 (m, 8H, H porphyrin phenyl ring); 8.76 (Hβ pyrrole, d, ^3J=4.6 Hz, 4H); 9.15 (Hβ pyrrole, d, ^3J=4.6 Hz, 4H); 9.92 (H *meso*, s, 2H). MS (FAB) (*m*/*z*): calcd for $C_{35}H_{24}N_4O_3^{102}Ru$ (M^+): 650.0898. Found: 650.0902. UV–VIS (CH_2Cl_2): $\lambda_{max/nm}$ (log ε): 398 (5.28); 517 (4.19). ν_{CO} 1936

4.3.3. 5,15-Bis(9,9′-spirobifluoren-2-yl)-2,8,12,18-tetraethyl-3,7,13,17-tetramethylporphyrinato ruthenium carbonyl 17. Yield: 75%. ^{1}H NMR ($CDCl_3$, ppm) (αα and αβ): δ 1.73 (CH_3 ethyl, t, 12H); 2.35 (CH_3 methyl, s, 12H); 3.84 (CH_2 ethyl, q, 8H); 6.69–6.91 (H spirobifluorene, m, 6H); 7.12 (H spirobifluorene, m, 4H); 7.36–7.58 (H spirobifluorene, m, 6H); 7.71 (H spirobifluorene, m, 4H); 7.94 (H spirobifluorene, m, 6H); 8.16 (H spirobifluorene, m, 4H); 9.84 ($H_{X,XX}$ *meso*, s, 2H). MS (ESI: CH_2Cl_2/MeOH: 9/1) (*m/z*): calcd for $C_{83}H_{64}N_4O^{102}Ru$ ($M^{\cdot+}$):1234.4124. Found: 1234.4170. UV–VIS (CH_2Cl_2): $\lambda_{max/nm}$ (log ε): 228 (4.84); 296 (4.47); 308 (4.50); 401 (5.01); 521 (3.99); 552 (3.90). IR (KBr, cm^{-1}): ν_{CO} 1938.

4.3.4. *meso*-5,10,15,20-Tetrakis(9,9′-spirobifluoren-2-yl)porphyrinato ruthenium carbonyl 21. Yield: 82%. ^{1}H NMR(toluene d_8, ppm) (4α, 3αβ,2α2β, αβαβ): 6.90 (H spirobifluorene, dd, 4H); 7.11–7.20 (H spirobifluorene, m, 12H), 7.22–7.30 (H spirobifluorene, m, 12H); 7.50–7.83 (H spirobifluorene, m, 16H); 7.9–8.33 (H spirobifluorene, m, 16H); 8.87 (H β pyrrole, m, 8H). MS (ESI: CH_2Cl_2/MeOH: 9/1) (*m/z*): calcd for $C_{121}H_{68}N_4ONa^{102}Ru$ ($M+Na^+$): 1717.4334. Found: 1717.4330. UV–VIS (CH_2Cl_2): $\lambda_{max/nm}$ (log ε): 228 (5.1); 298 (4.66); 309 (4.74); 420 (5.31); 533 (4.28); 569 (3.84). IR (KBr, cm^{-1}): ν_{CO} 1938. CV (CH_2Cl_2 0.2 M/Bu_4NPF_6, Fc/Fc^+): 0.46 V; 0.89 V; 1.37 V.

4.3.5. Typical procedure for phsophine ligation: 5,15-bis(9,9′-spirobifluoren-2-yl)porphyrinato ruthenium bis (methyl-diphenyl phosphine) 8. To a solution of ruthenium carbonyl complex (50 μmol) dissolved in distilled and degassed chloroform or dichloromethane was added methyldiphenylphosphine (300 μmol) under an argon atmosphere. The solution was stirred at room temperature until the reaction was completed (5 min). The bis-ligation was checked by monitoring the UV–VIS spectrum. After removal of the solvent, the crude product was crystallized in hexane or pentane to give the Ru(II)bis(methyldiphenylphosphine) complex (yield: 85%). ^{1}H NMR (toluene d_8, ppm) (αα and αβ): δ −2.64 (CH_3 phosphine, t, 1.5H); −2.36 (CH_3 phosphine, t, 3H); −2.14 (CH_3 phosphine, t, 1.5H); 4.19 (H phosphine *o*-phenyl ring, m, 2H); 4.25 (H phosphine *o*-phenyl ring, m, 4H); 4.41 (H phosphine *o*-phenyl ring, m, 2H); 5.96–6.31 (H phosphine *m*-phenyl ring, m, 8H); 6.45–6.61 (H phosphine *p*-phenyl ring, m, 4H); 6.96 (H spirobifluorene, m, 3H); 7.46–8.25 (H spirobifluorene, m, 27H); 8.51 (H *β* pyrrole, m, 4H); 8.69 (H *β*pyrrole, m, 4H); 9.17 ($H_{X,XX}$ *meso*, s, 1H); 9.21 ($H_{X,XX}$ *meso*, s, 1H). ^{31}P NMR (toluene d_8, ppm) (αα et αβ): 2.6 (P phosphine, 1P); 2.7 (P phosphine, 1P). MS (ESI: CH_2Cl_2/MeOH: 9/1) (*m/z*): calcd for $C_{96}H_{66}N_4P_2^{102}Ru$ ($M^{\cdot+}$):1438.3806. Found: 1438.3847. UV–VIS (CH_2Cl_2): $\lambda_{max/nm}$ (log ε): 426 (5.3); 510 (4).

4.3.6. 5,15-Bis(2-methoxyphenyl) porphyrinato ruthenium bis(methyl-diphenyl phosphine) 11. Yield: 85%. ^{1}H NMR ($CDCl_3$): αα isomer: δ − 2.37 (CH_3 phosphine, t, 3H); −2.15 (CH_3 phosphine, t, 3H); 3.74 (CH_3 methoxy group, s, 6H); 4.16 (H phosphine *o*-phenyl ring, m, 4H); 4.35 (H phosphine *o*-phenyl ring, m, 4H); 6.45 (H phosphine *m*-phenyl ring, m, 8H); 6.76 (H phosphine *p*-phenyl ring, m, 4H); 7.41–7.7 H porphyrin phenyl ring, m, 8H); 8.25 (H β pyrrole, d ^3J=4 Hz, 4H); 8.48 (H β pyrrole, d ^3J=4 Hz, 4H); 8.70 (H*meso*, s, 2H). αβ isomer: δ −2.24 (CH_3 phosphine, t, 6H); 3.68 (CH_3 methoxy group, s, 6H); 4.25 (H phosphine *o*-phenyl ring, m, 8H); 6.43 (H phosphine *m*-phenyl ring, t, 8H); 6.77 (H phosphine *p*-phenyl ring, t, 4H); 7.38–7.67 (H porphyrin phenyl ring, m, 8H); 8.27 (H β pyrrole, d ^3J=4.1 Hz, 4H); 8.45 (H β pyrrole, d ^3J=4.1 Hz, d, 4H); 8.68 (H*meso*, s, 2H). MS FAB (*m/z*): calcd for $C_{47}H_{37}N_4O_2P^{102}Ru$ ($M-P(Ph)_2CH_3^+$)=822.1721. Found: 822.1711. UV–VIS (CH_2Cl_2): $\lambda_{max/nm}$ (log ε): 423 (5.13), 507 (3.86).

4.3.7. 5,15-Bis(3-methoxyphenyl)porphyrinato ruthenium bis(methyl-diphenyl phosphine) 12. Yield: 84%. ^{1}H NMR ($CDCl_3$): δ −2.35 (CH_3 phosphine, t, 6H); 4.05 (CH_3 methoxy group, s, 6H); 4.15 (H phosphine *o*-phenyl ring, m, 8H); 6.50 (H phosphine *m*-phenyl ring, t, 8H); 6.81 (H phosphine *p*-phenyl ring, t, 4H); 7.32–7.85 (H porphyrin phenyl ring, m, 8H); 8.34 (H β pyrrole, d, ^3J=4.2 Hz, 4H); 8.65 (H β pyrrole, d, ^3J=4.2 Hz, 4H); 9.13 (H*meso*, s, 2H). MS FAB (*m/z*): calcd for $C_{47}H_{37}N_4O_2P^{102}Ru$ ($M-P(Ph)_2CH_3^+$)=822.1721. Found: 822.1711.

4.3.8. 5,15-Bis(9,9′-spirobifluoren-2-yl)-2,8,12,18-tetraethyl-3,7,13,17-tetramethyl porphyrinato ruthenium bis(methyl-diphenyl phosphine) 18. Yield: 85%. ^{1}H NMR ($CDCl_3$, ppm): (αα and αβ): δ −2.70 (CH_3 phosphine, t, 1, 5H); −2.54 (CH_3 phosphine, t, 3H); −2.30 (CH_3 phosphine, t, 1, 5H); 1.53 (CH_3 ethyl, m, 12H); 2.13 (CH_3 methyl, s, 12H); 3.60 (CH_2 ethyl, m, 8H); 3.80 (H phosphine *o*-phenyl ring, m, 2H); 4.02 (H phosphine *o*-phenyl ring, m, 4H); 4.12 (H phosphine, *o*-phenyl ring, m, 2H); 5.75 (H phosphine *m*-phenyl ring, m, 4H); 6.01–6.10 (H phosphine, *m*-phenyl ring, m, 4H); 6.26 (H phosphine *p*-phenyl ring, m, 2H); 6.39 (H phosphine, *p*-phenyl ring, m, 2H); 6.87–7.93 (Hspirobifluorene, m, 30H); 9 ($H_{X,XX}$ *meso*, s, 1H); 9.1 ($H_{X,XX}$ *meso*, s, 1H). ^{31}P NMR ($CDCl_3$, ppm) (αα and αβ): 3.14 (P phosphine, 1P); 3.16 (P phosphine, 1P). MS (ESI: $CHCl_3$/MeOH: 95/5) (*m/z*): calcd for $C_{108}H_{90}N_4P_2$ ^{102}Ru ($M^{\cdot+}$):1606.5715. Found: 1606.5707. UV–VIS (CH_2Cl_2): $\lambda_{max/nm}$ (log ε): 426 (5.10); 507 (4.2).

4.3.9. *meso*-5,10,15,20-Tetrakis(9,9′-spirobifluoren-2-yl)porphyrinato ruthenium bis(methyl-diphenyl phosphine) 22. Yield: 88%. ^{1}H NMR (toluene d_8, ppm) (4α, 3αβ, 2α2β, αβαβ): δ −2.90 (CH_3 phosphine, t, 0.37H); −2.64 (CH_3 phosphine, t, 1.5H); −2.36 (CH_3 phosphine, t, 1.5H); −2.31 (CH_3 phosphine, t, 0.75H); −2.04 (CH_3 phosphine, t, 1.5H); −1.82 (CH_3 phosphine, t, 0.37H); 4.09 (H phosphine, *o*-phenyl ring, m, 2H); 4.39 (H phosphine, *o*-phenyl ring, m, 4H); 4.50 (H phosphine, *o*-phenyl ring, m, 2H); 5.84 (H phosphine, *m*-phenyl ring, m, 2H); 6.12 (H phosphine *m*-phenyl ring, m, 6H); 6.52 (H phosphine, *p*-phenyl ring, m, 4H); 6.97–8.32 (H spirobifluorene+H β pyrrole, m, 68H). ^{31}P NMR (toluene d_8, ppm): 2.42 (s, br, 1P); 2.45 (s, br, 0.75P); 2.56 (s, 0.25P). UV–VIS (CH_2Cl_2): $\lambda_{max/nm}$ (log ε): 437 (5.43); 522 (3.47).

4.3.10. *meso*-5,10,15,20-Tetrakis(3-methylphenyl)-porphyrinato-rutheniumbis(methyl-diphenyl phosphine) 26. Yield: 85%. ^{1}H NMR ($CDCl_3$, ppm): δ −2.12 (CH_3 phosphine, t, 6H); 2.61 (CH_3, s, 12H); 4.34 (H phosphine *o*-phenyl ring, m, 8H); 6.51 (H phosphine *m*-phenyl ring, t, 8H); 6.80 (H phosphine *p*-phenyl ring, t,

4H); 7.32–7.8 (H porphyrin phenyl ring, m, 16H); 8.1 (H β pyrrole, s, 8H).

4.4. Typical procedure for isocyanide ligation

To a solution of ruthenium carbonyl complex (50 μmol) in distilled chloroform or dichloromethane was added *t*-butylisocyanide (300 μmol) under an argon atmosphere. The solution was stirred at room temperature until the reaction was completed. The bis-ligation was checked by monitoring the UV–VIS spectrum. After filtration, the solvents were removed under vacuum and the residue was dissolved in dichloromethane. Pentane was then added and the solution was set aside for one day for crystallization at 0 °C. Purple crystals of Ru(II) bis(*t*-butylisocyanide) complex were collected by filtration and washed with hexane.

4.4.1. 5,15-Bis(9,9′-spirobifluoren-2-yl)porphyrinato ruthenium bis(*t*-butylisocyanide) 9. Yield: 85%. ^{1}H NMR ($CDCl_3$, ppm) (αα and αβ): δ −0.99 (CH_3 *t*-BuNC, s, 4.5H); −0.76 (CH_3 *t*-BuCN, s, 9H); −0.64 (CH_3 *t*-BuCN, s, 4.5H); 6.86–7.77 (H spirobifluorene, m, 24H); 8.12 (H spirobifluorene, m, 6H); 8.43 ($H_{III,VII,XIII,XVII}$ β pyrrole, m, 4H), 8.75 ($H_{II,VIII,XII,XVIII}$, β pyrrole, d, 4H), 9.42 ($H_{X,XX}$ *meso*, s, 2H).MS (ESI: CH_2Cl_2/MeOH: 9/1) (*m*/*z*): calcd for $C_{80}H_{58}N_6{}^{102}Ru$ ($M^{\cdot+}$):1204.3766. Found: 1204.3780. UV–VIS (CH_2Cl_2): $\lambda_{max/nm}$ (log ε): 228 (5.10); 296 (4.73); 308 (4.75); 411 (5.28); 525 (3.98); 560 (3.59). IR (liquid, CH_2Cl_2, cm^{-1}): ν_{CN} 2219.

4.4.2. 5,15-Bis(2-methoxyphenyl) porphyrinato ruthenium bis(*t*-butylisocyanide) 13. Yield: 85%. ^{1}H NMR ($CDCl_3$, ppm): αα isomer δ −0.92 (CH_3 *t*-BuNC, s, 9H); −0.21 (CH_3 *t*-BuNC, s, 9H); 4.12 (CH_3 methoxy, s, 6H); 7.3–7.8 (H porphyrin phenyl ring, m, 8H); 8.91 (H β pyrrole, d ^3J=4 Hz, 4H), 9.15 (H, β pyrrole, d ^3J=4 Hz, 4H), 9.7 (H *meso*, s, 2H). αβ isomer: −0.58 (CH_3 *t*-BuNC, s, 18H); 4.07 (CH_3 methoxy, s, 6H); 7.3–7.8 (H phenyl ring, m, 8H); 8.43 (H β pyrrole, d ^3J=4 Hz, 4H), 8.75 (H, β pyrrole, d ^3J=4 Hz, 4H), 9.62 (H *meso*, s, 2H). ν_{CN}: 2112.

4.4.3. 5,15-Bis(3-methoxyphenyl) porphyrinato ruthenium bis(*t*-butylisocyanide) 14. Yield: 80%. ^{1}H NMR ($CDCl_3$, ppm): −0.62 (CH_3 *t*-BuNC, s, 18H); 4.2 (CH_3 methoxy, s, 6H); 7.3–7.8 (H porphyrin phenyl ring, m, 8H); 8.3 (H β pyrrole, d ^3J=4 Hz, 4H), 8.55 (H, β pyrrole, d ^3J=4.3 Hz, 4H), 9.82 (H *meso*, s, 2H). ν_{CN}: 2113.

4.4.4. 5,15-Bis(9,9′-spirobifluoren-2-yl)-2,8,12,18-tetraethyl-3,7,13,17-tetramethyl porphyrinato ruthenium bis(*t*-butylisocyanide) 19. Yield: 85%. ^{1}H NMR ($CDCl_3$, ppm) (αα and αβ): δ −0.94 (CH_3 *t*-BuCN, s, 4.5H); −0.70 (CH_3 *t*-BuCN, s, 9H); − 0.58 (CH_3 *t*-BuCN, s, 4.5H); 1.62 (CH_3 ethyl, m, 12H); 2.30 (CH_3 methyl, s, 12H); 3.74 (CH_2 ethyl, m, 8H); 7.07–8.12 (H spirobifluorene, m, 30H); 9.39 ($H_{X,XX}$ *meso*, s, 2H). MS (ESI:$CHCl_3$/MeOH: 95/5) (*m*/*z*): calcd for $C_{92}H_{82}N_6{}^{102}Ru$ ($M^{\cdot+}$): 1372.5671. Found: 1372.5702. UV–VIS (CH_2Cl_2): $\lambda_{max/nm}$ (log ε): 228 (4.92); 296 (4.56); 308 (4.58); 411 (5.11); 520 (3.86); 560 (3.40). IR (KBr, cm^{-1}): ν_{CN} 2113.

4.4.5. *meso*-5,10,15,20-Tetrakis(9,9′-spirobifluoren-2-yl)-porphyrinato-ruthenium bis(*t*-butylisocyanide) 23. Yield: 90%. ^{1}H NMR ($CDCl_3$, ppm) (4α, 3αβ, 2α2β, αβαβ): δ-1.18 (CH_3 *t*-BuCN, s, 1.1H); −0.96 (CH_3 *t*-BuCN, s, 4.5H); −0.86 (CH_3 *t*-BuCN, s, 2.25H); −0.74 (CH_3 *t*-BuCN, s, 4.5H); −0.62 (CH_3 *t*-BuCN, s, 4.5H); −0.50 (CH_3 *t*-BuCN, s, 1.1H); 6.88 (H spirobifluorene, d, 4H); 7.02 (H spirobifluorene, m, 8H), 7.18 (H spirobifluorene, m, 12H); 7.30–7.51 (H spirobifluorene, m, 16H); 7.70 (H spirobifluorene, t, 8H); 8.02 (H spirobifluorene, m, 12H); 8.12 (H β pyrrole, m, 8H). MS (ESI: CH_2Cl_2/MeOH: 9/1) (*m*/*z*): calcd for $C_{130}H_{86}N_6{}^{102}Ru$ ($M^{\cdot+}$): 1832.5957. Found: 1832.6014. UV–VIS (CH_2Cl_2): $\lambda_{max/nm}$ (log ε): 227 (5.21); 297 (4.68); 307 (4.7); 425 (5.52); 532 (3.55). IR (KBr, cm^{-1}): ν_{CN} 2107.

4.4.6. *meso*-5,10,15,20-Tetrakis(3-methylphenyl)porphyrinato-ruthenium bis(*t*-butylisocyanide) 27. Yield: 90%. ^{1}H NMR ($CDCl_3$, ppm) −0.41 (CH_3 *t*-BuNC, s, 18H); 2.65 (CH_3, s, 12H); 7.6 (H porphyrin phenyl ring, m, 8H); 8.01 (H porphyrin phenyl ring, m, 8H); 8.47 (H β pyrrole, s, 8H).

Acknowledgements

We thank MESRT support for CP. Dr. J. Rault-Berthelot and Dr. A. Bondon were very helpful in the obtention and discussion of voltammograms and NMR spectra, respectively.

References and notes

1. Kim, Y. H.; Shin, D. C.; Kim, S. H.; Ko, C. H.; Yu, H. S.; Chae, Y. S.; Kwon, S. K. *Adv. Mater.* **2001**, *13*, 1690–1693.
2. Zeng, G.; Yu, W. L.; Chua, S. J.; Huang, W. *Macromolecules* **2002**, *35*, 6907–6914.
3. Chiang, C. L.; Shu, C. F. *Chem. Mater.* **2002**, *14*, 682–687.
4. Lee, H.; Oh, J.; Chu, H. Y.; Lee, J. I.; Kim, S. H.; Yang, Y. S.; Kim, G. H.; Do, L. M.; Zyung, T.; Lee, J.; Park, Y. *Tetrahedron* **2003**, *59*, 2773–2779.
5. Prelog, V.; Bedekovic, D. *Helv. Chim. Acta* **1979**, *62*, 2285–2302.
6. Wu, F.; Riesgo, E. C.; Thummel, R. P.; Juris, A.; Hissler, M.; El-ghayoury, A.; Ziessel, R. *Tetrahedron Lett.* **1999**, *40*, 7311–7314.
7. Aviram, A. *J. Am. Chem. Soc.* **1988**, *110*, 5687–5692.
8. Farazdel, A.; Dupuis, M.; Clementi, E.; Aviram, A. *J. Am. Chem. Soc.* **1990**, *112*, 4206–4214.
9. Rault-Berthelot, J.; Granger, M. M.; Mattiello, L. *Synth. Met.* **1998**, *97*, 211–215.
10. Lorcy, D.; Mattiello, L.; Poriel, C.; Rault-Berthelot, *J. Electroanal. Chem.* **2002**, *530*, 33–39.
11. Poriel, C.; Ferrand, Y.; Le Maux, P.; Rault-Berthelot, J.; Simonneaux, G. *J. Chem. Soc., Chem. Commun.* **2003**, 1104–1105.
12. Osuka, A.; Ida, K.; Maruyama, K. *Chem. Lett.* **1989**, 741–744.
13. Wu, R.; Schumm, J. S.; Pearson, D. L.; Tour, J. M. *J. Org. Chem.* **1996**, *61*, 6906–6921.
14. Winter-Werner, B.; Diederich, F.; Gramlich, V. *Helv. Chim. Acta* **1996**, *79*, 1338–1360.
15. Pei, J.; Ni, J.; Zhou, X. H.; Cao, X. Y.; Lai, Y. H. *J. Org. Chem.* **2002**, *67*, 4924–4936.

16. Mattielo, L.; Fioravanti, G. *Synth. Commun.* **2001**, *31*, 2645–2648.
17. Arsenault, G. P.; Bullock, E.; MacDonald, S. F. *J. Am. Chem. Soc.* **1960**, *82*, 4384.
18. Manka, J. S.; Lawrence, D. S. *Tetrahedron Lett.* **1989**, *30*, 6989–6992.
19. Littler, B. J.; Miller, M. A.; Hung, C. H.; Wagner, R. W.; O'Shea, D. F.; Boyle, P. D.; Lindsey, J. S. *J. Org. Chem.* **1999**, *64*, 1391–1396.
20. Medforth, C. J. *The Porphyrin Handbook*; Kadish, K. M., Smith, K. M., Guilard, R., Eds.; Academic: San Diego, 2000; Vol. 5, p 65.
21. Le Maux, P.; Bahri, H.; Simonneaux, G. *J. Chem. Soc., Chem. Commun.* **1991**, 1350–1352.
22. Vicente, M. G. H.; Nurco, D. J.; Shetty, S. J.; Medforth, C. J.; Smith, K. M. *J. Chem. Soc., Chem. Commun.* **2001**, 483–484.
23. Bonifazi, D.; Diederich, F. *J. Chem. Soc., Chem. Commun.* **2002**, 2178–2179.
24. Young, R.; Chang, C. K. *J. Am. Chem. Soc.* **1985**, *107*, 898–909.
25. Le Maux, P.; Bahri, H.; Simonneaux, G. *Tetrahedron* **1993**, *49*, 1401–1408.
26. Gunter, M. J.; Mander, L. N. *J. Org. Chem.* **1981**, *46*, 4792–4795.
27. Poriel, C.; Ferrand, Y.; Le Maux, P.; Rault-Berthelot, J.; Simonneaux, G. *Tetrahedron Lett.* **2003**, *44*, 1759–1761.
28. Collman, J. P.; Gagne, R. R.; Reed, C. A.; Halbert, T. H.; Lang, G.; Robinson, W. T. *J. Am. Chem. Soc.* **1975**, *97*, 1427–1439.
29. Gottwald, L. K.; Ullman, E. F. *Tetrahedron Lett.* **1969**, 3071–3074.
30. Setsune, J. I.; Hashimoto, M.; Shiozawa, K.; Hayakawa, J.; Ochi, T.; Masuda, R. *Tetrahedron* **1998**, *54*, 1407–1424.
31. Jaquinod, L. *The Porphyrin Handbook*; Kadish, K. M., Smith, K. M., Guilard, R., Eds.; Academic: San Diego, 2000; Vol. 1, pp 201–237.
32. Ogoshi, H.; Saita, K.; Saturai, K. I.; Watanabe, T.; Toi, H.; Ayoma, Y. *Tetrahedron Lett.* **1986**, *27*, 6365–6368.
33. Sanders, G. M.; van DIijk, M.; Machiels, B. M.; van Veldhuisen, A. *J. Org. Chem.* **1991**, *56*, 1301–1305.
34. Nierengarten, J. F.; Oswald, L.; Nicoud, J. F. *J. Chem. Soc., Chem. Commun.* **1998**, 1545–1546.
35. Darling, S. L.; Goh, P. K. Y.; Bampos, N.; Feeder, N.; Montalti, M.; Prodi, L.; Johnson, B. F. G.; Sanders, J. K. M. *J. Chem. Soc., Chem. Commun.* **1998**, 2031–2032.
36. Poriel, C.; Ferrand, Y.; Le Maux, P.; Paul, C.; Rault-Berthelot, J.; Simonneaux, G. *Chem. Commun.* **2003**, 2308–2309.
37. Kost, D.; Carlson, E. H.; Raban, M. *Chem. Commun.* **1971**, 656–657.
38. Gilman, H.; Kirby, J. E.; Kinney, C. R. *J. Am. Chem. Soc.* **1929**, *51*, 2252–2261.
39. Lash, T. D. *Tetrahedron* **1998**, *54*, 359–374.